

Chelating dihydroxamic acids: study of metal speciation and co-ordination compounds with Ni²⁺ and Cu²⁺

Jolanta Świątek-Kozłowska,^{*a} Igor O. Fritsky,^{*b} Agnieszka Dobosz,^a Aldona Karaczyn,^c Nikolai M. Dudarenko,^b Tatiana Yu. Sliva,^b Elżbieta Gumienka-Kontecka^c and Lucjan Jerzykiewicz^c

^a Department of Basic Medical Sciences, Wrocław Medical University, Kochanowskiego 14, 51-601 Wrocław, Poland. E-mail: jsk@basmed.am.wroc.pl

^b Department of Chemistry, Shevchenko University, 01033 Kiev, Ukraine. E-mail: kokozay@chem.kiev.ua

^c Faculty of Chemistry, University of Wrocław, F. Joliot-Curie 14, 50-383 Wrocław, Poland

Received 10th July 2000, Accepted 6th September 2000

First published as an Advance Article on the web 18th October 2000

Solution (potentiometric, absorption, EPR) as well as solid state studies (X-ray, EPR, magnetic susceptibility) have shown that the binding ability of oxalodihydroxamic acid (H₂oxha) with two hydroxamic groups next to each other differs distinctly from that observed for aliphatic dihydroxamic acids, HONHOC(CH₂)_nCONHOH (*n* = 3–8). H₂oxha was found to be a very powerful ligand for Ni^{II} and Cu^{II} due to an *N,N'*-chelating binding mode. The availability of the mixed nitrogen–oxygen donor systems results in formation of polymeric complexes with Cu^{II}. The crystal structure of K₂[Ni(oxha)₂]·2H₂O has shown two very characteristic features of the dihydroxamic ligand: (i) two short intramolecular hydrogen bonds stabilising very effectively the complex formed and (ii) very specific binding modes of K⁺ ions, which play a bridging role between [Ni(oxha)₂]²⁻ ions. The latter finding demonstrates a capacity of H₂oxha-based anionic complex species to form polynuclear complexes with different bridging modes.

Aliphatic dihydroxamic acids HONHOC(CH₂)_nCONHOH with *n* = 3–8 were intensively studied in solution with respect to their complexation properties towards metal ions.¹ In these ligands two donor hydroxamic groups are separated by the polymethylene bridge, which prevents them forming chelate cycles with participation of both hydroxamic groups. Therefore, their donor properties in fact do not differ from those characteristic for monohydroxamic acids. In particular, most typical for this class of ligands is a *O,O'*-chelating bonding mode, and N-bonding with substitution of the NH proton by a metal ion does not occur in solution or in the crystal state.

In our recent research we paid special attention to the role of the adjacent donor group in attempts to achieve N-bonding of the hydroxamic function.^{2,3} Three types of such additional donor groups which facilitate N-bonding of hydroxamate are known: amino (both aromatic and aliphatic), phenolic and oxime groups. One can conclude that N-bonding of hydroxamate can occur provided a strong additional donor group is present which can form a stable chelate ring with participation of the hydroxamate nitrogen. A second hydroxamic group situated close enough to the first one to form a 5- or 6-membered chelate ring would be suitable to satisfy this requirement. However, the donor properties of such ligands (dihydroxamic acids with *n* = 0 or 1, *i.e.* oxalodihydroxamic acid (H₂oxha) and malonodihydroxamic acid) have not been studied profoundly. In spite of extensive solution studies of complex formation with dihydroxamic acids,¹ the mentioned ligands remain largely unexplored. Only a solution study of H₂oxha with Fe³⁺ ions was reported.⁴ H₂oxha was used as a coolant ingredient of propellants, and this led to its extensive study by structural methods.⁵ However, only one crystal structure of a metal complex (thallium(I)) with this ligand is reported to date.⁶

The present paper reports a study of co-ordination ability of H₂oxha with Ni²⁺ and Cu²⁺ ions both in solution and in the solid state. It appeared to be a very powerful chelating agent towards these metal ions and exhibited the *N,N'*-chelating bonding mode in a number of species formed in neutral and

alkaline solution. Moreover, H₂oxha belongs to the family of oxamide-derived ligands, which has extensively been explored as regards molecular magnetism.⁷ Taking into account that both hydroxamic and oxamide moieties can play a bridging function between metal ions, one might expect the formation of versatile bi- or poly-nuclear complexes and co-ordination polymers with this ligand.

Experimental

Preparations

All chemicals were commercial products of reagent grade used without further purification. Elemental analyses (C,H,N) were conducted by the Microanalytical Service of the University of Wrocław. The ligand H₂oxha was prepared according to the reported method⁸ using diethyl oxalate.

Cu(oxha)·H₂O 1. The compound Cu(NO₃)₂·H₂O (0.242 g, 1 mmol) dissolved in water (10 cm³) was added to an aqueous solution (15 cm³) of H₂oxha (0.240 g, 2 mmol). The dirty dark green precipitate formed immediately, was filtered off, washed with water and ethanol and dried in vacuum. Yield 0.17 g (85%). The complex is virtually insoluble in water and all common organic solvents. Calc. for C₂H₄CuN₂O₃: C, 12.03; H, 2.02; Cu, 31.84; N, 14.03. Found: C, 11.71; H, 1.76; Cu, 32.04; N, 13.64%. IR (cm⁻¹): 885, 1021 (N–O_{hydroxamic}); 1587 (C=N_{hydroxamic}); 1638 (C=O, Amide I); 3242, 3430br (O–H).

K₂[Ni(oxha)₂]·2H₂O 2. The compound Ni(NO₃)₂·6H₂O (0.291 g, 1 mmol) dissolved in ethanol (15 cm³) was added to an aqueous solution (15 cm³) of H₂oxha (0.240 g, 2 mmol). Potassium hydroxide (0.235 g, 4.2 mmol) dissolved in 15 cm³ of ethanol was then added. The resulting solution was left at 0 °C for 3 h, then the precipitated potassium nitrate was filtered off and the filtrate allowed to crystallise at room temperature in the air. Red-orange needle crystals were separated by filtration after 36 h. Yield 0.23 g (56%). Calc. for C₄H₈K₂N₄NiO₁₀: C, 11.75; H,

1.97; N, 13.70; Ni, 14.35. Found: C, 11.50; H, 2.16; N, 14.03; Ni, 14.09%. IR (cm^{-1}): 880, 1020 (N–O_{hydroxamic}); 1600 (C=N_{hydroxamic}); 1630 (C=O, Amide I); 3260br (O–H).

Potentiometric studies

Stability constants for proton, copper(II) and nickel(II) complexes were calculated from titration curves carried out at 25 °C using sample volumes of 1.5 cm³. Alkali was added from a 0.250 cm³ micrometer syringe, which was calibrated by both weight titration and the titration of standard materials. The metal ion concentration was 1×10^{-3} mol dm⁻³ and the metal-to-ligand ratios were 1:2, 1:3, 1:4 and 1:6. The pH-metric titrations were performed at 25 °C in 0.1 mol dm⁻³ KNO₃, on a MOLSPIN pH-meter system using a Russel CMAW 711 semi-micro combined electrode calibrated in hydrogen ion concentrations using HNO₃.⁹ Three titrations were performed for each molar ratio, and the SUPERQUAD computer program was used for stability constant calculations.¹⁰ Standard deviations quoted were computed by SUPERQUAD, and refer to random errors only. They are, however, a good indication of the importance of a particular species in the equilibrium.

Spectroscopic and magnetochemical studies

Diffuse reflectance spectra of solid samples were obtained on a Beckman UV 5240 spectrometer. Absorption spectra of solutions were recorded on a Beckman DU 650 spectrophotometer. The metal-ion concentrations were 3×10^{-3} mol dm⁻³ and metal-to-pro-ligand ratios of 1:1, 1:2 and 1:5. The EPR spectra were recorded on a Bruker ESP 300E spectrometer at X-band (9.3 GHz) at 120 K, in ethane-1,2-diol–water (1:2). Concentrations used in the spectroscopic measurements were similar to those given for potentiometric titrations. Infrared spectra (KBr pellets) were recorded on a Perkin-Elmer 180 Spectrometer in the range 400–4000 cm⁻¹. Variable-temperature magnetic susceptibility data (2–300 K) were acquired on a powdered sample with use of a Quantum Design MPMS-5 SQUID magnetometer. Corrections for the diamagnetism of the ligand were applied using Pascals constants. The results of potentiometric, UV–VIS and EPR spectroscopy studies are given in Table 1.

X-Ray crystallography

Details of the crystal data and refinement for compound **2** are given in Table 2. Data were collected on an KUMA KM-4 diffractometer¹¹ with graphite-monochromated Mo-K α radiation ($\lambda = 0.71073$ Å) using the ω -2 θ technique. Corrections were made for Lorentz-polarisation and absorption¹² effects. There was no crystal decay as measured by three standard reflections. The structure was solved by direct methods (SHELXS 97),¹³ and refined by full-matrix least squares (SHELXL 97)¹⁴ anisotropically for all non-hydrogen atoms. All hydrogen atoms were located from Fourier difference maps and refined isotropically without any restraints.

CCDC reference number 186/2176.

See <http://www.rsc.org/suppdata/dt/b0/b005500j/> for crystallographic files in .cif format.

Results and discussion

Solution studies

Two dissociation constants corresponding to stepwise ionisation of hydroxamic groups ($\text{p}K_{\text{a}1} = 6.740(2)$ and $\text{p}K_{\text{a}2} = 8.684(2)$) were found for H₂oxha, close to those reported previously.⁴ The first constant is nearly three orders of magnitude lower than the typical values for aliphatic monohydroxamic acids¹⁵ and about one and a half orders lower than $\text{p}K_{\text{a}1}$ of 2-(hydroxyimino)propanohydroxamic acid (H₂poha) (8.16).^{2,3} This is indicative of the relatively strong electron withdrawing

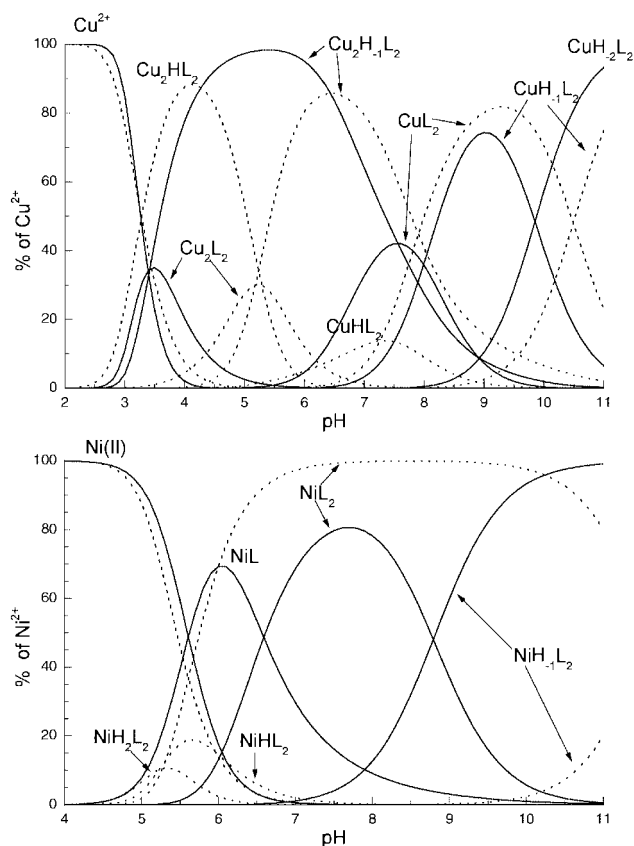


Fig. 1 Species distribution diagram for Cu²⁺–H₂L (a) and Ni²⁺–H₂L (b) at 25 °C and $I = 0.1$ mol dm⁻³ KNO₃. Concentration of ligand 0.003 mol dm⁻³ and concentration of metal ions 0.006 mol dm⁻³. H₂oxha, solid line; H₂poha, dotted line.

effect of the second hydroxamic group as compared to the oximic group. The monoprotonated species can additionally be stabilised by an intramolecular hydrogen bond O–H...O=C; this effect may also contribute to the lowering of $\text{p}K_{\text{a}1}$ and increase of $\text{p}K_{\text{a}2}$.

The distribution diagrams of complex species for Cu²⁺ and Ni²⁺ evaluated from the potentiometric calculations are presented in Fig. 1a,b. The corresponding stability constants are given in Table 1. Comparison of the values of the stability constants for the similar species formed by H₂oxha and H₂poha reveals that those for the complex species of the former ligand are 6.5–10.5 (for Ni²⁺) and 2–5.5 (for Cu²⁺) orders of magnitude lower than those observed in H₂poha systems. Nevertheless, H₂oxha appeared to be a stronger chelating agent. In both Ni²⁺ and Cu²⁺ systems the concentration of the free metal ions begins to drop at a relatively low pH value, in a pattern very similar to that of with H₂poha (Fig. 1).

In the Cu²⁺–H₂L system EPR spectra are absent in the pH range 3.5–6.5 which is consistent with formation of the dimeric species evaluated from potentiometric measurements (Fig. 1a). Two dimeric species, [Cu₂L₂] and [Cu₂H₋₁L₂]⁻, are formed in this range of pH. Absorption spectra (Table 1) suggest the presence of at least two nitrogens in equatorial co-ordination in both complexes. This means that in [Cu₂L₂] both nitrogen atoms of the ligands are deprotonated, and the only way for co-ordination of the second copper ion is bridging *via* the amide oxygen atoms (Scheme 1, a). Deprotonation of [Cu₂L₂] (with $\text{p}K_{\text{a}} = 3.42$) leads to formation of [Cu₂H₋₁L₂]⁻. Such a low value of the dissociation constant clearly indicates changing of the bridging mode: deprotonation of the OH group of one of the hydroxamic functions facilitates the (O,O') hydroxamic bridge (Scheme 1, b). Note, that no [Cu₂HL₂]⁺ species was detected (unlike with H₂poha) which is connected with impossibility for the protonated amide group to be co-ordinated.

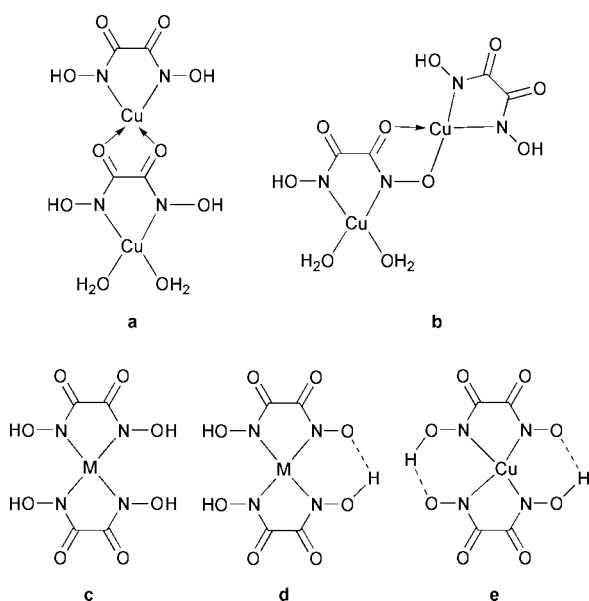
Table 1 Spectroscopic (UV–Vis and EPR) and potentiometric data for H₂L–Ni²⁺ and H₂L–Cu²⁺ systems in metal-to-ligand molar ratio 2:1, at 25 °C and *I* = 0.1 mol dm⁻³ KNO₃

Species	log β	log β for H ₂ poha species	λ _{max} /nm	ε/dm ³ mol ⁻¹ cm ⁻¹	A _η /T × 10 ⁴	g _η
HL	8.684(2)	11.00(6)				
H ₂ L	15.424(2)	19.16(7)				
NiL	7.07(2)	—	^a		—	—
NiL ₂	12.82(2)	22.16(1)	496	261	—	—
NiH ₋₁ L ₂	4.04(4)	10.56(3)	455	343	—	—
CuL ₂	18.22(6)	22.65(5)	575	117	205.4	2.25
CuH ₋₁ L ₂	10.22(8)	12.16(5)	521	157	210.4	2.26
CuH ₋₂ L ₂	0.37(12)	—	510	227	215.1	2.25
			750	27		
Cu ₂ L ₂	26.17(9)	31.84(8)	^a		—	—
Cu ₂ H ₋₁ L ₂	22.75(6)	26.66(6)	588	189	—	—

^a Precipitation.

Table 2 Crystal data and structure refinement for complex **2**

Empirical formula	C ₂ H ₄ KN ₂ Ni _{0.5} O ₅
<i>M</i>	204.53
<i>T</i> /K	299(1)
Crystal system	Monoclinic
Space group	<i>P</i> 2 ₁ / <i>n</i>
<i>a</i> /Å	3.7290(10)
<i>b</i> /Å	19.753(4)
<i>c</i> /Å	8.203(2)
β/°	101.91(3)
<i>U</i> /Å ³	591.2(2)
<i>Z</i>	4
μ/mm ⁻¹	2.410
Measured/independent reflections	1138/1012
[<i>R</i> (int)]	[0.0147]
Final <i>R</i> 1, <i>wR</i> 2 indices [<i>I</i> > 2σ(<i>I</i>)]	0.0234, 0.0647
(all data)	0.0299, 0.0738



Scheme 1 Suggested structures for [Cu₂L₂] **a**, [Cu₂H₋₁L₂]⁻ **b**, [ML₂]²⁻ **c**, [MH₋₁L₂]³⁻ **d** and [CuH₋₂L₂]⁴⁻ **e** (*M* = Cu²⁺ or Ni²⁺).

Above pH 6.0 the monomeric species begin to be formed: [CuL₂]²⁻, [CuH₋₁L₂]³⁻, and [CuH₋₂L₂]⁴⁻. In the Ni²⁺ containing system only two similar monomeric species are formed: [NiL₂]²⁻ and [NiH₋₁L₂]³⁻. Absorption spectral data for both Ni²⁺ and Cu²⁺ complexes and EPR parameters for Cu²⁺ complexes indicate that the monomeric bis complexes are square-planar MN₄ species. The stepwise dissociation constants in both Ni²⁺ and Cu²⁺ series of monomeric species (8.0–9.85 log

units) are close to the deprotonation constant of the hydroxamic group and *cis*-disposed oxime groups in square-planar Ni²⁺ and Cu²⁺ complexes.^{2,3} Ionisation of OH groups in given species may be promoted by formation of short intramolecular hydrogen bonds between *cis*-disposed oxygen atoms. Stepwise deprotonation is accompanied by notable shortwave shifts of the d–d absorption maxima and increase of the corresponding ε values in both Ni²⁺ and Cu²⁺ systems, although all species preserve the MN₄ mode (Table 1). A similar effect of a short intramolecular hydrogen bond in bis-oximate complexes was observed before in a Cu²⁺–2-hydroxyiminopropanamide system.^{16a} Thus, the bonding modes presented in Scheme 1, **c,d,e** can be ascribed.

The comparison of species' distributions for Ni²⁺ and Cu²⁺ systems with H₂oxha and H₂poha shows that in the case of the dihydroxamic acid all the similar species start to be formed and reach maximum abundance at noticeably lower values of pH. The distribution curves for H₂oxha are shifted towards lower pH values as compared to those for H₂poha. The reason for this is that the amide groups in the presence of Ni²⁺ and Cu²⁺ ions are deprotonated at markedly lower pH values than the oxime groups.¹⁶ However, the general metal binding ability of the ligands is almost identical as shown by the very similar decrease of free metal ion concentration with pH increase (Fig. 1).

Synthesis and solid state study

Interaction of H₂oxha with solutions of copper(II) salts in the pH region 3–10 (regardless of ligand:metal ratio) results in formation of a dark green precipitate of composition Cu(oxha)·H₂O **1**. The complex is not soluble in water and common organic solvents and is sure to have a polymeric structure. At the concentrations applied in potentiometric and UV–VIS studies (30–100 times lower than those applied in synthesis), solutions remained clear for several hours, presumably due to slow formation of polymeric species or oversaturation. In more concentrated solutions used in synthesis, polymerisation appears to be more favourable, and an insoluble product is formed immediately. Only on addition of an excess of alkali (pH > 10) to a solution with a 1:2 metal-to-ligand ratio is it possible to obtain a clear reddish brown solution containing square-planar complex species (Scheme 1, **c–e**). However, isolation of the solid complexes seemed not to be successful due to ligand degradation because of hydrolysis of the hydroxamic function to carboxylate. Similar behaviour of copper(II) complexes with H₂poha in alkaline solutions was observed.³ In contrast, alkaline solutions containing nickel(II) salts and H₂oxha in 1:2 molar ratio are hydrolytically stable, and we succeeded in isolating the complex K₂[Ni(oxha)₂]·2H₂O **2** in crystalline state.

The diffuse reflectance spectrum of complex **1** contains two

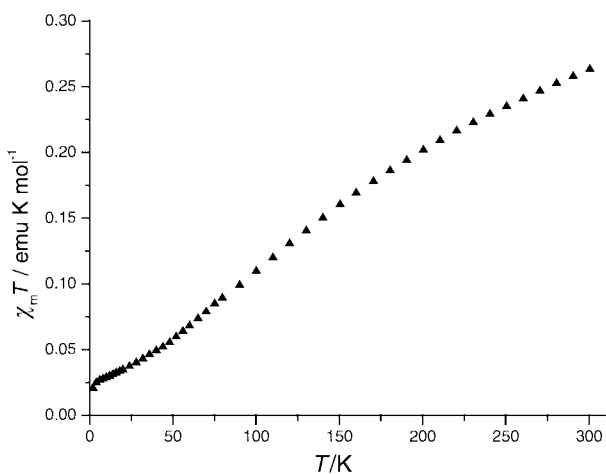


Fig. 2 Temperature dependence of $\chi_m T$ (per Cu atom) for complex 1.

maxima in the visible region (408 and 603 nm). The first is probably due to charge transfer and cannot be ascribed to a d-d transition; the latter suggests the presence of copper(II) ions in a mixed nitrogen and oxygen environment. The temperature dependence of χT for **1** is shown in Fig. 2. The observed room temperature value of χT (0.263 emu K mol⁻¹) is significantly lower than expected for non-interacting copper(II) species. This, together with a smooth decrease of χT on cooling (down to 2.07×10^{-2} emu K mol⁻¹ at 2.1 K) is indicative of strong antiferromagnetic interactions in the complex. However, attempts to interpret the observed susceptibility in terms of the Bonner–Fischer model for linear chains were not successful, and a regular polymeric chain structure for **1** has been ruled out. The shape of the curve and the range of the observed χT values are reminiscent of reported *trans*-oxamidatocopper(II) complexes consisting of interacting dimeric units having $J = 300\text{--}600$ cm⁻¹ due to a very effective transmission of exchange interaction between paramagnetic ions by oxamidato bridges.^{7,17} Thus, one can suggest that **1** comprises interacting dimeric units maintained by oxamide or hydroxamic bridges (Scheme 1, a, b), and the co-ordination spheres of the copper atoms are complemented by additional bonds with donor oxygen atoms of adjacent dimers and water molecules. This conclusion is supported by the similarity of the EPR spectrum of **1** to those observed for other reported copper(II) complexes containing weakly interacting *trans*-oxamido bridged dimers.¹⁷ The EPR spectrum of a powdered sample of **1** at room temperature exhibits a slightly asymmetric feature with $g = 2.08$ and no signal at half-field. On cooling, the signal decreases in intensity but does not indicate any clear anisotropy. We tried to fit the observed susceptibility data using a modified Bleaney–Bowers equation for a two-dimensional network of interacting dimers, which takes into account the intermolecular exchange,^{17a,c} but convergence was not achieved, indicating the presence of additional interactions between dimeric units or an oligomeric structure in **1**.

The molecular structure and the numbering scheme for compound **2** is presented in Fig. 3, and selected bond parameters are given in Table 3. **2** comprises the complex anions [Ni(oxha)₂]²⁻, potassium cations and the water molecules of solvation. The central atom in the complex anion is in a specific position, so that the anion is centrosymmetric. It is surrounded in square-planar mode by four nitrogen donor atoms belonging to the N-deprotonated hydroxamic groups. The co-ordinated dianions of the dihydroxamic acid still carry O-protonated hydroxamic functions. The Ni–N bond lengths (1.863(2) and 1.873(2) Å) are typical for square-planar nickel(II) complexes with deprotonated amide ligands;^{3,16b,c} the chelate angle N(1)–Ni–N(2) is 81.13(10)°. In fact, the linear parameters of the co-ordination sphere are very close to those observed in the complex [Ni(poha)₂]²⁻.³ In the co-ordinated dihydroxamate

Table 3 Selected bond lengths (Å) and angles (°) for complex 2

Ni–N(1)	1.873(2)	K–O(1) ⁽ⁱⁱⁱ⁾	2.783(2)
Ni–N(2)	1.863(2)	K–O(1) ^(iv)	2.813(2)
O(1)–C(1)	1.258(3)	K–O(2)	2.758(2)
O(2)–C(2)	1.240(3)	K–O(2) ⁽ⁱⁱ⁾	2.692(2)
O(3)–N(1)	1.416(3)	K–O(2) ^(iv)	2.828(2)
O(4)–N(2)	1.421(3)	K–O(4)	3.018(2)
N(1)–C(1)	1.301(4)	K–O(5)	2.772(2)
N(2)–C(2)	1.312(4)	K...K ⁽ⁱⁱ⁾	3.7290(10)
C(1)–C(2)	1.524(4)		
N(1)–Ni–N(1) ⁽ⁱ⁾	180.0	O(1)–C(1)–C(2)	120.4(2)
N(1)–Ni–N(2)	81.13(10)	N(1)–C(1)–C(2)	110.8(2)
N(1) ⁽ⁱ⁾ –Ni–N(2)	98.87(10)	O(2)–C(2)–N(2)	128.9(2)
C(1)–N(1)–O(3)	113.8(2)	O(2)–C(2)–C(1)	121.3(2)
C(2)–N(2)–O(4)	114.6(2)	N(2)–C(2)–C(1)	109.7(2)
O(1)–C(1)–N(1)	128.8(2)		

Symmetry transformations: (i) $-x, -y, -z$; (ii) $x - 1, y, z$; (iii) $x - \frac{3}{2}, -y - \frac{1}{2}, z - \frac{1}{2}$; (iv) $x - \frac{1}{2}, -y - \frac{1}{2}, z - \frac{1}{2}$; (v) $x + 1, y, z$; (vi) $x + \frac{3}{2}, -y - \frac{1}{2}, z + \frac{1}{2}$; (vii) $x + \frac{1}{2}, -y - \frac{1}{2}, z + \frac{1}{2}$.

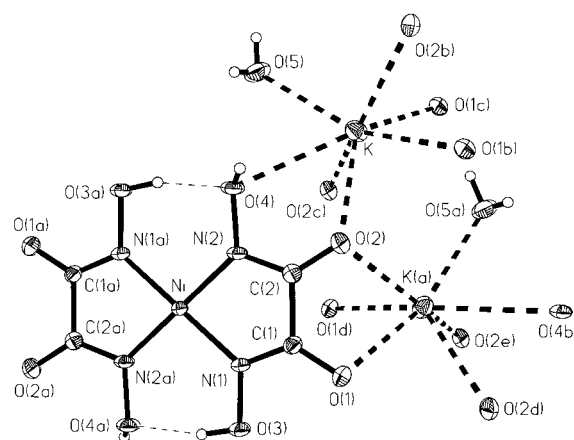


Fig. 3 Molecular structure and numbering scheme for complex 2.

the C–O, N–O and C–N bond lengths indicate unambiguously the presence of the functional groups in hydroxamic rather than oximic form.³

The main principal structural differences between [Ni(oxha)₂]²⁻, and [Ni(poha)₂]²⁻ are in the peculiarities of the short intramolecular hydrogen bonds. In the present complex both *cis*-disposed hydroxamic oxygen atoms carry hydrogen atoms, which differ in their orientations. One of them is *cis* with respect to the neighbouring oxygen atom and forms a short hydrogen bond with it and the second is *trans* and forms a hydrogen bond with one of the solvate water molecules. The intermolecular hydrogen bond is distinctively asymmetric (O(3)–H 0.92(6), H...O(4a) 1.74(6) Å), and the O...O separation (2.64(3) Å) is noticeably longer than values typical for *cis*-oximate complexes (1.43–1.48 Å). Note that in [Ni(poha)₂]²⁻ containing a heteroleptic short hydrogen bond formed both by hydroxamic and deprotonated oxime groups this separation is only 2.503(3) Å.

Planar nickel(II) complex anions are packed in columns (Fig. 4) perpendicularly to the x axis with Ni...Ni(1 + x, y, z) separations of 3.729(1) Å. The columns are related by translations along the z direction of the crystal and form walls lying parallel to the xz plane. Translational columns are linked by hydrogen bonds formed by water molecule O(5) with amide and hydroxamic oxygens. Potassium cations are co-ordinated to the oxygen donor atoms of four complex anions belonging to two different walls related by translations in the y direction (Fig. 5). Co-ordination occurs in three different modes: O(1)(amide), O(2)(amide) chelating, O(2)(amide), O(4) (hydroxamic) chelating, O(1)(amide) and O(2)(amide) monodentate. The fact that potassium cations were found to play a bridging function between nickel(II) complex anions in two different chelate

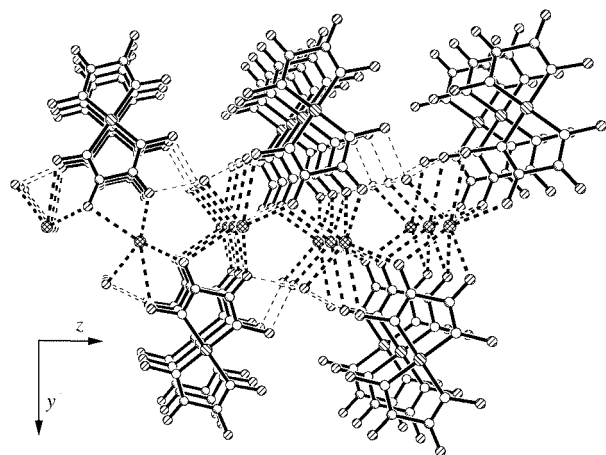


Fig. 4 Packing diagram for complex **2** (projection on yz plane). Potassium co-ordination bonds are depicted with thick dashed lines, hydrogen bonds with thin dashed lines.

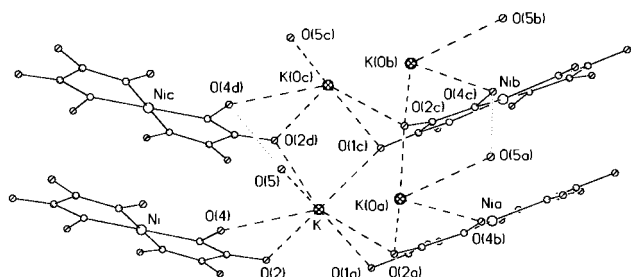
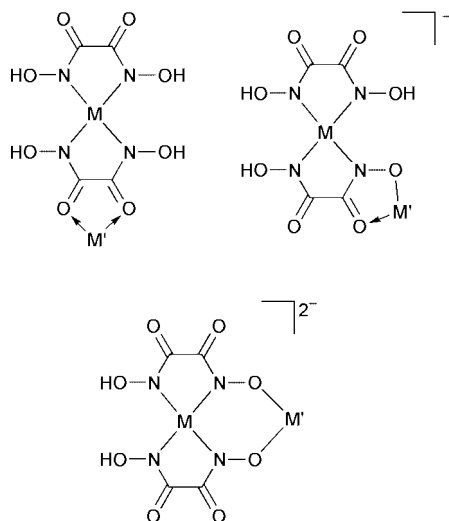


Fig. 5 Fragment of the crystal structure of complex **2** demonstrating co-ordination of potassium cations.



Scheme 2 Possible bridging co-ordination of metal ions to complex anions $[ML_2]^{2-}$, $[MH_{-1}L_2]^{3-}$ and $[MH_{-2}L_2]^{4-}$ ($M = Cu^{2+}$ or Ni^{2+} , $M' =$ cation of divalent metal).

modes, namely forming oxamide and hydroxamic bridges (Fig. 3), demonstrates a capacity of H_2Oxha -based anionic complexes to form polynuclear complexes with extended bridges of high nuclearity. The co-ordination number of the potassium cation is increased to seven by water molecule O(5); the bond distances are in the range 2.692(2)–3.018(2) Å, which is normal for potassium cations.¹⁸ Thus, potassium cations form frameworks parallel to the xz plane, which are inserted between translational anionic walls (Fig. 4). The $K \cdots K$ separations in the framework are 3.729(1) (in direction x) and 4.190(1) Å (in direction z).

Conclusion

Two adjacent hydroxamic functions form a very effective set of

donors, which is able to bind Cu^{II} and Ni^{II} via N, N' and mixed nitrogen–oxygen donor sets. Anionic complexes with N, N' co-ordination to Cu^{II} and Ni^{II} exhibit remarkable ability to co-ordinate additional metal ions in two different bridging modes, which makes them very promising building blocks for obtaining magnetically coupled polynuclear assemblies (Scheme 2).

Acknowledgements

This work was performed within the COST action D8 and partially supported by a grant from the Wrocław Medical University (project 519) and University of Wrocław. T. Yu. S. thanks the Royal Society of Chemistry for a grant within the Programme *Journals Grants for International Authors*.

References

- B. Kurzak, H. Kozłowski and E. Farkas, *Coord. Chem. Rev.*, 1992, **114**, 169; B. Kurzak, L. Nakonieczna, G. Rusek, H. Kozłowski and E. Farkas, *J. Coord. Chem.*, 1993, **28**, 17; D. A. Brown, R. A. Coogan, N. J. Fitzpatrick, W. K. Glass, D. E. Abukshima, L. Shiels, M. Ahlgren, K. Smolander, T. T. Pakkanen, T. A. Pakkanen and M. Perakyla, *J. Chem. Soc., Perkin Trans. 2*, 1996, 2673.
- A. Dobosz, I. O. Fritsky, A. Karaczyn, H. Kozłowski, T. Yu. Sliva and J. Świątek-Kozłowska, *J. Chem. Soc., Dalton Trans.*, 1998, 1089.
- A. Dobosz, N. M. Dudarenko, I. O. Fritsky, T. Głowiak, A. Karaczyn, H. Kozłowski, T. Yu. Sliva and J. Świątek-Kozłowska, *J. Chem. Soc., Dalton Trans.*, 1999, 743.
- D. Monnier and C. Jegge, *Helv. Chim. Acta*, 1957, **40**, 513; Z. Krych and T. Lipiec, *Ann. Acad. Med. Lodz.*, 1967, **9**, 247.
- C. K. Lowe-Ma and D. L. Decker, *Acta Crystallogr., Sect. C*, 1986, **42**, 1648; A. S. Begum, V. K. Jain, C. L. Khetrapal and N. C. Shivaprakash, *J. Crystallogr. Spectrosc. Res.*, 1987, **17**, 545; A. S. Begum, V. K. Jain, S. Ramakumar and C. L. Khetrapal, *Acta Crystallogr., Sect. C*, 1988, **44**, 1047.
- S.-H. Huang, R.-J. Wang and T. C. W. Mak, *J. Chem. Soc., Dalton Trans.*, 1991, 1379.
- C. Diaz, J. Ribas, R. Costa, J. Tercero, M. S. El Fallah, X. Solans and M. Font-Bardia, *Eur. J. Inorg. Chem.*, 2000, **4**, 675; O. Cadour, C. Mathoniere and O. Kahn, *Inorg. Chem.*, 1997, **36**, 1923; J. L. Sanz, B. Cervera, R. Ruiz, C. Bois, J. Faus, F. Lloret and M. Julve, *J. Chem. Soc., Dalton Trans.*, 1996, 1359; C. Mathoniere, O. Kahn, J. C. Daran, H. Hilbig and F. H. Koehler, *Inorg. Chem.*, 1993, **32**, 4057.
- C. R. Hauser and W. B. Renfrow, in *Org. Synth.*, 1943, **Coll. Vol. 2**.
- P. Gans, A. Sabatini and A. Vacca, *J. Chem. Soc., Dalton Trans.*, 1985, 1195.
- H. M. Irving, M. H. Miles and L. D. Pettit, *Anal. Chim. Acta*, 1967, **68**, 475.
- Kuma KM4 software, Kuma Diffraction, Wrocław, 1998.
- P. Starynowicz, COSABS 99, Program for Absorption Correction, University of Wrocław, 1999.
- G. M. Sheldrick, *Acta Crystallogr., Sect. A*, 1990, **46**, 467.
- G. M. Sheldrick, SHELXL 97, Program for the Refinement of Crystal Structures, University of Göttingen, 1997.
- L. Bauer and O. Exner, *Angew. Chem., Int. Ed. Engl.*, 1974, **13**, 376.
- (a) C. O. Onindo, T. Yu. Sliva, T. Kowalik-Jankowska, I. O. Fritsky, P. Buglyo, L. D. Pettit, H. Kozłowski and T. Kiss, *J. Chem. Soc., Dalton Trans.*, 1995, 3911; (b) T. Yu. Sliva, T. Kowalik-Jankowska, V. M. Amirkhanov, T. Głowiak, Ch. O. Onindo, I. O. Fritsky and H. Kozłowski, *J. Inorg. Biochem.*, 1997, **65**, 287; (c) A. M. Duda, A. Karaczyn, H. Kozłowski, I. O. Fritsky, T. Głowiak, E. V. Prisyazhnaya, T. Yu. Sliva and J. Świątek-Kozłowska, *J. Chem. Soc., Dalton Trans.*, 1997, 3853.
- (a) J. M. Dominguez-Vera, N. Galvez, E. Colacio, R. Cuesta, J.-P. Costes and J. P. Laurent, *J. Chem. Soc., Dalton Trans.*, 1996, 861; (b) J. A. Real, R. Ruiz, J. Faus, J. F. Lloret, M. Julve, Y. Journaux, M. Philoche-Levisalle and C. Bois, *J. Chem. Soc., Dalton Trans.*, 1994, 3769; (c) Z.-N. Chen, H.-X. Zhang, C.-Y. Su, Z.-Y. Zhou, K.-Ch. Zheng and B.-S. Kang, *Inorg. Chem.*, 1998, **37**, 3877; (d) A. Bencini, C. Beneli, A. C. Fabretti, G. Franchini and D. Gatteschi, *Inorg. Chem.*, 1986, **25**, 1063.
- I. O. Fritsky, H. Kozłowski, P. J. Sadler, O. P. Yefetova, J. Świątek-Kozłowska, V. A. Kalibabchuk and T. Głowiak, *J. Chem. Soc., Dalton Trans.*, 1998, 3269; V. Kh. Kravtsov, O. N. Rebrova, Yu. A. Simonov, R. D. Lampeka and I. O. Fritskii, *Russ. J. Inorg. Chem. (Engl. Transl.)*, 1992, **37**, 743.